Computer Aided Diagnosis for CT Colonography via Slope Density Functions

Gabriel Kiss, Johan Van Cleynenbreugel, Paul Suetens, and Guy Marchal

Faculties of Medicine & Engineering
Medical Image Computing (Radiology - ESAT/PSI)
University Hospital Gasthuisberg
Herestraat 49, B3000 Leuven, BELGIUM
Gabriel.Kiss@uz.kuleuven.ac.be

Abstract. The paper presents a system for Computer Aided Detection in Virtual Colonography based on geometric modeling. We label locations in the CT volume data, which have a high probability of being colonic polyps, and present them in a user-friendly way. We introduce a method for fast colonic wall elimination and then model polyps based on Slope Density Functions, to be able to reduce the number of false positive cases. The method was tested on a study group of 50 data sets. Using normal colonoscopy as standard of reference, true positive and false positive findings were determined. The detection rate for polyps larger than 6mm was above 85%. Initial results show that Computer Aided Diagnosis is feasible and that our method holds potential for screening purposes.

1 Introduction

Colorectal cancer is amongst the leading causes of cancer related death in the industrialized world, with a 4-6% lifetime risk in the general population [1]. Fortunately colorectal cancer is characterized by slow growth (5-10 years), likely evolution including the appearance of adenomatous polyps. The malignancy of these structures increases with increasing size. As a result early detection and treatment of colonic neoplasms can prevent colonic cancer. Studies [2] show that the survival rate after five years is 92% when early treatment is received. That is why screening for colorectal cancer has received increasing attention.

Many detection methods are available, including fecal occult blood testing (FOBT), barium enema examinations, sigmoidoscopy, colonoscopy, virtual colonography and lately genetic testing. From the mentioned methods only FOBT was used in screening. Although safe and inexpensive, it has a low sensitivity and thus effectiveness. Colonoscopy on the other hand has the highest accuracy and it is widely considered as a gold standard, but it is invasive and costly. Lately CT colonography (CTC) has been proposed as a possible alternative for screening. Introduced in 1994 by Vining et. al. [3], it is a method for exploring the colonic area hinging on CT data.

With the appearance of the 16 slice multi-slice CT machines the number of acquired slices is well beyond 1000 per patient, especially if two scans per

R.E. Ellis and T.M. Peters (Eds.): MICCAI 2003, LNCS 2878, pp. 746–753, 2003.
© Springer-Verlag Berlin Heidelberg 2003

patient (prone and supine) are acquired. It is not difficult to see that perceptual errors due to human fatigue can affect the performance of CT colonography. To overcome this problem, automated methods for polyp detection were developed. Computer Aided Detection (CAD) is a possible approach to improve reading efficiency and accuracy. It consists in automatic detection of conspicuous masses that resemble polyps.

The remaining of the paper is organized as follows: first our method for CAD is presented followed by results on 50 colonoscopic datasets. The advantages and pitfalls of the method are presented in the discussion section. Finally some conclusions on the future of CAD are presented.

2 Method

Although it is a new research field several approaches have been already proposed [4,5,6,7]. What our method tries to achieve is to eliminate as much of the colonic wall as possible, as quickly as possible and without loosing interesting locations (polyps). It tries to do that by a simple geometric trick and then applies a more elaborate algorithm on the remaining structures to come up with the final candidates. Our primary goal is to detect protruded, polypoid type neoplasms larger than 5 mm.

Our method has two main steps: generation where the voxels belonging to the colonic wall are determined, followed by a fast elimination of the voxels belonging to normal wall and a testing step which uses a model based approach (employing slope density functions) to eliminate the remaining false positive detections.

2.1 Generation

Segmentation. In this step the colonic wall is determined. Since CTC images have a large contrast between (insufflated) colonic air and colonic wall, classic region growing algorithms [8], with multiple seed points (to overcome collapsed regions) can be used successfully. Automatic threshold computation is done using the cumulative Laplacian histogram of the image volume [9]. A detailed description of the threshold selection process can be found in [7]. The final result of the segmentation algorithm is thus the set of disjunctive regions representing voxels on the colonic wall.

Colonic wall elimination. When looking at the structure of the colon one can easily observe that most of it is concave. Fortunately, polypoid structures have a convex appearance, thus clearly distinguishable from the normal wall. One problem that arises is that haustral folds have also a convex but cylindrical appearance.

The principle of our method is presented in figure 1. For each voxel, the colonic wall is intersected with the plane α perpendicular to the local surface normal and situated at a distance d from the surface of the wall. The resulting patterns of intersection can be seen in figure 2. As highlighted in the figure the

colonic wall gives completely filled planes while polyps and folds give a smaller number of voxels in the reformatted plane. Thus to eliminate the colonic wall we propose a thresholding method based on the number of voxels in the reformatted plane (in fact in a squared region of n pixels). The required number of pixels in the reformatted plane (expressed as a percentage of n^2) 70% and the distance $d = 1.5mm$ were determined empirically in order to ensure maximal response on polyps of 5 mm or larger.

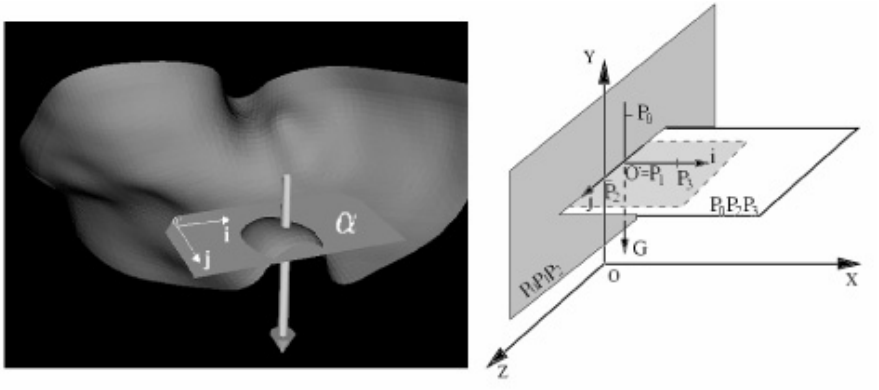

Fig. 1. Part of the colonic surface intersected with the plane α, on the right the coordinate system and main vectors used for extracting the voxels of the cut plane.

Analytically our method can be described as follows (see figure 1 (right) for details): given $P_0 = [x_0, y_0, z_0]^T$ as the current colonic point, compute $P_1 = [x_1, y_1, z_1]^T$ as $P_1 = P_0 + d.G$, where $G = [g_x, g_y, g_z]$ is the local gradient in P_0. Let α be the plane having the normal $\overrightarrow{P_0P_1}$ and $P_1 \in \alpha$. Consider P_2 as the intersection of the plane α with one of the axes of the global coordinate system $(Oxyz)$ and P_3 a point along the normal in P_1 to the plane $(P_0P_1P_2)$. The local coordinate system is fully determined by the points $P_1 \equiv O$', P_2 and P_3. The vectors $\overrightarrow{P_1P_2}$ and $\overrightarrow{P_1P_3}$ are normalized, thus obtaining the axes $\overrightarrow{O'i}$ and $\overrightarrow{O'j}$ of the coordinate system. The x, y, z coordinates of a point V having the local coordinates v_i, v_j are obtained as follows: $\overrightarrow{OV} = \overrightarrow{Ov_i} + \overrightarrow{Ov_j} - \overrightarrow{OO'}$.

2.2 Testing

After the concave colonic wall was eliminated the remaining regions are considered for further investigation. For that a shape-based classification is used. The actual statistical model building is described in the next section, here it will be shown how polyps are modeled and how a set of existing models are used for discriminating between normal and polypoid structures.

Slope density functions. We are modeling polyps based on their slope density function (SDF) [8]. The SDF can be seen as the histogram of gradient orienta-

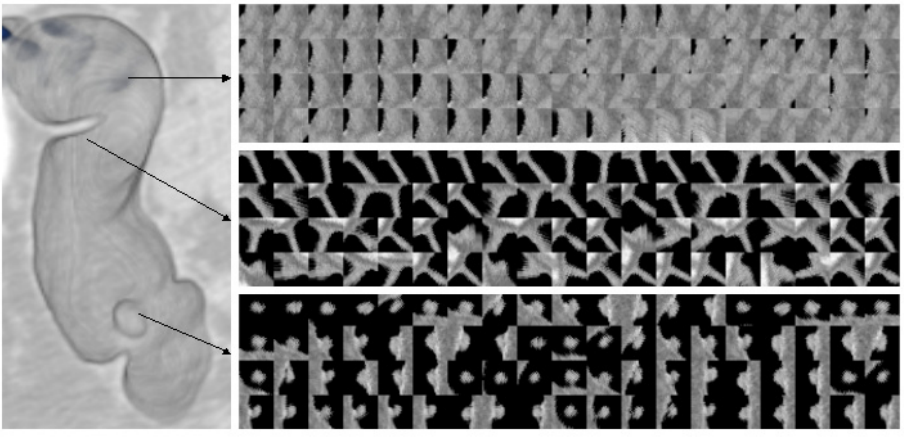

Fig. 2. Right patterns of intersection on the surface of the colon corresponding to: wall (top), fold (middle) and polyp (bottom). On the left thin slabs view of the colonic wall.

tions and while it is smooth for circular and elliptic objects, it shows peaks for elongated structures. That is why it can be used for discriminating between polyps and haustral folds.

Because no interpolation was done when extracting the reformatted planes (due to time efficiency), the irregularities in the extracted plane have to be eliminated. To compensate for them, the gradients in the reformatted plane are computed using the recursive filtering method of R. Deriche [10]. Using the recursive filtering method, it is easy to compute the Hessian of the image H, and thus the local curvature (k) on the boundary; $k = \frac{-t^T Ht}{\| \vec{g} \|}$, t-unit tangent vector. Typically boundaries contain parts belonging to the polypoid structure but additionally parts belonging to the colonic wall (figure 3), this having a negative effect on the SDF (mainly smoothing). To compensate for it all the points on the boundary having a negative curvature value are eliminated.

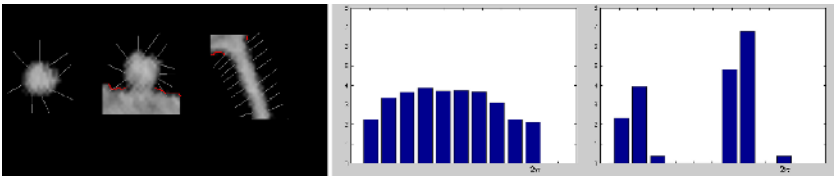

Fig. 3. Smoothed cut through two polyps and a haustral fold respectively. Gradient orientation and regions with negative curvature are indicated. SDF models corresponding to polyps and haustral folds are presented; they are used for classification purposes.

Sample modeling. In the training stage a set of SDF samples are presented to the classification algorithm, which will try to find similarities between them and group them into different clusters. From each cluster of samples a representative

model is built, thus we will have model SDF's for polyps, haustral folds and remaining colonic wall. In the testing step the distances between the SDF of the current point and the SDF's of the models are computed and the type of the current point is assigned to the type of the closest SDF.

The distance between SDF's is the χ^2 statistic, minimized over all discretized orientations. It is defined as:

$$D_{ij} = min\left(\sum_{k=1}^{K} \frac{[h_i((k+l)\%K) - h_j(k)]^2}{h_i((k+l)\%K) + h_j(k)}\right),\ l = 1..K \tag{1}$$

where $h(k)$ denotes the k-th element in the SDF histogram and l is the rotational coefficient.

Polyp extraction. After the previous step some positions on the colonic surface are labeled as polyp candidates. Of course multiple responses for the same polyp are obtained and on the other hand some responses are generated by noise (false positives). To eliminate these inconveniences a connected component extraction of final polyp candidates is employed.

In this step clusters of polyp labeled positions are identified. The connectedness is not limited to the first order neighbors but to all neighbors situated at a distance $d_{neighbor} < T_{neighbor}$, where $T_{neighbor} = 2$ (in our experiments) is a predefined constant.

Finally the mean position of the elements present in a cluster, having a number of components higher than $T_{component}$ is returned as a polyp candidate. The corresponding axial and 3D volume rendered positions are presented to the reading radiologist.

3 Polyp Models

3.1 Model Building

Suppose that a set of SDF's belonging to locations resulting after applying the generation step is available. To achieve a clustering of the training SDF samples a technique that produces a partition of the input according to a given distance is needed. The unsupervised learning algorithm proposed by Hutchinson in 1994 [11] can be considered a viable choice. It can be seen as a statistical clustering since it is based on numerical similarity within the object descriptions, in our case the SDF's. All one has to keep in mind at this moment is that the algorithm provides clusters of similar SDF's given a set of training samples.

Starting from the clusters returned by the algorithm models are built. Inside a cluster each sample contributes to the final model in a gaussian manner. By that centrally placed samples gain a higher weight than samples situated at the extremities of the cluster.

Before presenting the formula for the gaussian weights and the one used for the actual model computation, let's consider n the number of samples in the current cluster. The following notations can be introduced:

$$avgDist(i) = \frac{1}{n}\sum_{j=1}^{n} D_{ij};\ minDist = min(avgDist(i)),\ i = 1..n$$
$$totalDist = \sum_{i=1}^{n} avgDist(i);\ \sigma^2 = \frac{1}{n}\sum_{i=1}^{n}(avgDist(i) - minDist)^2$$

where $avgDist(i)$ is the average distance from the current sample to the remaining samples in the current cluster, and D_{ij} defined by equation 1.

The gaussian weight of each sample is given by:

$$G(i) = \frac{1}{\sigma.\sqrt{2\pi}} e^{-\frac{(avgDist(i)-minDist)^2}{2\sigma^2}}$$

The model is computed using the equation:

$$M_c(k) = \sum_{i=1}^{n} \frac{G(i)}{\sum_{j=1}^{n} G(j)} * h_i((k + l_i)\%K),\ k = 1..K \tag{2}$$

where l_i is a rotation coefficient used to minimize $totalDist$ over the current cluster c.

3.2 Hierarchical Classifier

Having a large number of training samples it is not feasible due to both memory and computation limitations to handle such an amount of data. Our solution was to split up the training data in groups of sn samples apply the clustering technique to each of them and then consider the resulting models as input to a higher level classification scheme. One problem that arises is that initial clusters and thus generated models have a different number of elements. This has to be accounted for when building models at higher levels. Considering Ell(i) as the number of pairs from which a certain model was attained, the modified model building equation can be rewritten as:

$$M_c(k) = \sum_{i=1}^{n} \frac{G(i).Ell(i)}{\sum_{j=1}^{n} G(j).\sum_{j=1}^{n} Ell(j)} * h_i((k + l_i)\%K),\ k = 1..K \tag{3}$$

We are aware of the fact that when using a hierarchical scheme some of the coarse details are lost, however this approach can be seen as a good compromise between accuracy and computational efficiency.

4 Results

Fifty CT colonographic data-sets, 25 normal and 25 with 40 polyps of various sizes (Table 1) were analyzed using the previously described CAD scheme. Informed consent was obtained from all patients and conventional colonoscopic findings were available. The patient preparation consisted in the oral administration of 3 to 5 liter of precolon, an in-house developed tagging agent. In some cases the use of polyethylene glycol electrolyte solution was preferred. Immediately before CT colonography a bowel relaxant was injected intravenously. CO2 was insufflated using a bag system.

Table 1. Polyp distribution and detection results. (No = total number of polyps, TP = true positives)

Adenoma type	No	Submerged	Detectable	TP	Sensitivity
Flat	6	1	5	1	20.00%
< 5 mm	8	2	6	2	33.33%
6-9 mm	10	3	7	6	85.70%
> 9 mm	12	1	11	10	90.90%
Tumor	4	0	4	4	100.00%
Total	40	7	33	23	69.69%

CT colonography was performed on a multi-detector CT (Multi Slice Helical CT; Volume Zoom, Siemens, Erlangen, Germany) using 4x1 mm detector configuration, 7 mm table feed per 0.5 s tube rotation, 0.8 mm reconstruction increment as well as 60 effective mAs and 120 keV. Patients were scanned in both supine and prone positions, in breadth holds of 20 to 30 seconds. The image processing was done on a dual processor, Intel Pentium 2.4 GHz system, having 2GB of RAM.

Using conventional colonoscopy as standard of reference true positive (TP) and false positive (FP) findings were determined for each patient. The detection rate differentiated on polyp size is presented in Table 1. The average computation time for the whole CAD process as well as for different steps is shown in Table 2.left. The total number of false positives was 124 on all the 50 data-sets, which gives us a mean value of 2.48 false positive findings per data-set. The main causes for false positives are presented in Table 2.right.

Table 2. Average computation times (expressed in minutes:seconds) and false positive causes in percent

Segmentation	0:11
Generation + Testing	4:07
Polyp extraction	0:07
Overall	4:25

Cause	Percent
Haustral fold	60.68 %
Colonic wall	18.80 %
Stool or fluid	11.97 %
Insuflation tube	5.13 %
Ileocecal valve	3.42 %

5 Discussion and Conclusion

In this paper a fast method for CAD in CT colonography was presented. The fastness of the method comes from reducing the shape-based analysis from a 3D space into a 2D space while preserving 3D clues. Its main purpose is the detection of polypoid lesions larger than 5mm. The results are obtained in less than 5 minutes a significant improvement over our previous scheme, which took 15 minutes to complete. On the relatively small database of patients it was proven that it has a high accuracy in detecting sessile and pedunculated polyps that protrude inwards into the lumen. It also can detect tumors, but has a low sensitivity for small polyps and for flat lesions.

Looking at the drawbacks of the method one can observe that the segmentation process is not fully automatic and that the pixel values around or inside the polyp are not taken into account. The reason for both is patient preparation and more explicitly fluid tagging. For the segmentation we preferred a semi-interactive step to ensure that a correct segmentation is achieved, and as much of the small bowel as possible is eliminated. The reason for not using pixel-based features is that some of our polyps are close to tagged colonic fluid or even semi-submerged and thus missed by such schemes.

Improvements of our scheme will include the generation of new polypoid models, learning from mistakes and the extension of the distance presented in equation 1, to include more 3D features. The main goal of our developments will be to further reduce the number of false positive findings.

The results of our experiments show that CAD in CT colonography is feasible, and a high sensitivity and specificity can be obtained. However to be relevant the tests have to be confirmed on a larger number of cases. Once its efficacy is proven, CAD can be integrated into clinical practice, improving on current accuracy and cost values.

Acknowledgement. This work is part of the GOA/99/05 project: "Variability in Human Shape and Speech", financed by the Research Fund, K.U. Leuven, BELGIUM. We would like to thank Maarten Thomeer for his involvement in the project.

References

1. Stevenson, G.: Radiology in the Detection and Prevention of Colorectal Cancer. Eur. J. Cancer. 31A (1995) 121–1126
2. Colorectal cancer – Oncology Channel. http:// www.oncologychannel.com /colon-cancer/
3. Vining, D.J., et al.: Virtual colonoscopy. Radiology (1994) 193:446 (abstract)
4. Summers, R.M., et al.: An Automated Polyp Detector for CT Colonography – Feasibility Study. Radiology (2000) 284–290
5. Gokturk, S.B., et al.: A Statistical 3-D Patter Processing Method for Computer-Aided Detection of Polyps in CT Colonography. IEEE Transactions on Medical Imaging (2001) 1251–1260
6. Yoshida, H., Nappi, J.: 3-D Computer-Aided Diagnosis Scheme for Detection of Colonic Polyps. IEEE Transactions on Medical Imaging (2001) 1261–1274
7. Kiss, G., et al.: Computer Aided Detection of Colonic Polyps via Geometric Features Classification. Proceedings 7th International Workshop on Vision, Modeling, and Visualization (2002) 27–34
8. Ballard, D.M., Brown, C.M.: Computer Vision. Prentice Hall (1982) 123–166
9. Wiemker R., Pekar, V.: Fast Computation of Isosurface Contour Spectra for Volume Visualization. Proceedings Computer Assisted Radiology and Surgery CARS (2001)
10. Deriche, R.: Fast Algorithms for Low-Level Vision. IEEE Transactions on Pattern Analysis and Machine Intelligence (1990) 78–87
11. Unsupervised learning http://www.cs.mdx.ac.uk /staffpages /serengul /ML /unsupervised.html